Tolerance and Long-Term MRI Imaging of Gadolinium-Modified Meshes Used in Soft Organ Repair

Vincent Letouzey, Stéphanie Huberlant, Arnaud Cornille, Sébastien Blanquer, Olivier Guillaume, Laurent Lemaire, Xavier Garric, Renaud de Tayrac

PLOS | ONE

RESEARCH ARTICLE

Tolerance and Long-Term MRI Imaging of Gadolinium-Modified Meshes Used in Soft Organ Repair

Vincent Letouzey[1]*, Stéphanie Huberlant[1], Arnaud Cornille[1], Sébastien Blanquer[2], Olivier Guillaume[2], Laurent Lemaire[3], Xavier Garric[2], Renaud de Tayrac[1]

1 Department of Obstetrics and Gynecology, Nîmes University Hospital, Place du Pr R. Debré, 30000, Nîmes, France, **2** Department of Artificial Polymers, Max Mousseron Institute of Biomolecules, CNRS UMR 5247, 34000, Montpellier, France, **3** Institut National de la Santé et de la Recherche Médicale, UMR-S 1066, MINT, 49000, Angers, France

* vincent.letouzey@chu-nimes.fr

OPEN ACCESS

Citation: Letouzey V, Huberlant S, Cornille A, Blanquer S, Guillaume O, Lemaire L, et al. (2015) Tolerance and Long-Term MRI Imaging of Gadolinium-Modified Meshes Used in Soft Organ Repair. PLoS ONE 10(3): e0120218. doi:10.1371/journal.pone.0120218

Academic Editor: Ichio Aoki, National Institute of Radiological Sciences, JAPAN

Received: October 16, 2014

Accepted: January 20, 2015

Published: March 26, 2015

Data Availability Statement: All relevant data are within the paper.

Funding: The authors received no specific funding for this work.

Competing Interests: Vincent Letouzey, Stephanie Huberlant, Arnaud Cornille, Sébastien Blanquer, Olivier Guillaume, Laurent Lemaire and Xavier Garric have no financial disclaimer or conflict of interest to declare. Renaud de Tayrac is consultant for Boston Scientific, Aspide Medical, Sofradim-Covidien, AMS,

Abstract

Background

Synthetic meshes are frequently used to reinforce soft tissues. The aim of this translational study is to evaluate tolerance and long-term MRI visibility of two recently developed Gadolinium-modified meshes in a rat animal model.

Materials and Methods

Gadolinium-poly-ε-caprolactone (Gd-PCL) and Gadolinium-polymethylacrylate (Gd-PMA) modified meshes were implanted in Wistar rats and their tolerance was assessed daily. Inflammation and biocompatibility of the implants were assessed by histology and immunohistochemistry after 30 days post implantation. Implants were visualised by 7T and 3T MRI at day 30 and at day 90. Diffusion of Gadolinium in the tissues of the implanted animals was assessed by Inductively Coupled Plasma Mass Spectrometry.

Results

Overall Gd-PMA coated implants were better tolerated as compared to those coated with Gd-PCL. In fact, Gd-PMA implants were characterised by a high ratio collagen I/III and good vascularisation of the integration tissues. High resolution images of the coated mesh were obtained *in vivo* with experimental 7T as well as 3T clinical MRI. Mass spectrometry analyses showed that levels of Gadolinium in animals implanted with coated mesh were similar to those of the control group.

Conclusions

Meshes coated with Gd-PMA are better tolerated as compared to those coated with Gd-PCL as no signs of erosion or significant inflammation were detected at 30 days post implantation. Also, Gd-PMA coated meshes were clearly visualised with both 7T and 3T MRI

Coloplast, Ethicon, and Allergan. This does not alter the authors' adherence to all PLOS ONE policies.

devices. This new technique of mesh optimisation may represent a valuable tool in soft tissue repair and management.

Introduction

Synthetic meshes have been routinely used for soft tissue reinforcement since their introduction in late 1950s [1]. Although hernia and abdominal wall repair is the most common application, reconstructive surgery and in particular pelvic organ prolapse (POP) repair are practiced in a large number of patients with success rates going up to 90% for the cystocele repair [2,3].

Meshes can be classified according to their properties including pore size and fiber type [4], weight and biomaterial composition [5].

Those commonly used in clinical practice are made of: (i) macroporous polypropylene (PP), which is a non-absorbable material; (ii) polyester (PET); polytetrafluoroethylene (PTFE) and expanded PTFE, etc. [6, 7]. Randomised prospective trials have underlined the interest of the treatment by synthetic meshes in terms of quality, low postoperative morbidity and long-term results, balanced with the recurrence of surgery due to mesh complication [8,9].

Indeed, for POP repair a prevalence of 15 to 20% of short-medium-term mesh complications (more than 6 months) is reported. These include pain, discomfort, vaginal bleeding, abnormal discharge, and recurrence of the prolapse that may eventually necessitate implant removal [10,11]. For hernia and abdominal wall repair common complications are chronic pain, seroma and adhesions [12,13].

Therefore, it is essential to optimise the mesh in order to improve tolerance and biocompatibility to the implant. Also, to improve management of complications and reduce recurrence of surgery, monitoring the position or a possible shrinkage of the implants would be a considerable advantage. Also, the possibility to visualise the mesh may be helpful for its removal following a complication. Magnetic resonance imaging (MRI) seems to be the most powerful imaging technique for the pelvic exploration [14,15]. Unfortunately, PP meshes are not spontaneously visible in MRI and the interposition of fascia makes the demarcation of implants impossible [16]. We previously described a method to covalently bind gadolinium to resorbable (poly(ε-caprolactone), PCL) and non-resorbable (poly(methyl acrylate), PMA) polymers and then coat the resulting Gd-polymers onto PP meshes. With this approach we obtained a satisfactory visualisation of the optimised meshes in experimental (*in vitro*) and clinical (*in vivo*) MRI [17]. With the present study we sought to evaluate (i) the preclinical tolerance and (ii) long-term MRI visibility of the previously described Gadolinium-modified PP meshes.

To this purpose we used a rat animal model, which is one of the preferred animal model for mesh fascia repair research [18–20] and two distinct method of implantation: (i) within the abdominal wall to assess the tolerance and biocompatibility and (ii) dorsal implantation to evaluate MR imaging.

Materials and Methods

Animals and surgical procedure and evaluation of clinical tolerance

In vivo experiments were performed at Nîmes University Hospital. The study was approved by the appropriate Animal Research Ethics Committee (CEEA-LR-1010) and conducted according to European Union animal care guidelines (Directive 2010/63/EU). All rats were female, 9–10 weeks old and weighed more than 300 g (mean 355 g ± 40g). The animals were housed on a 12:12-hour light–dark cycle and food and water were available ad libitum. All animals were

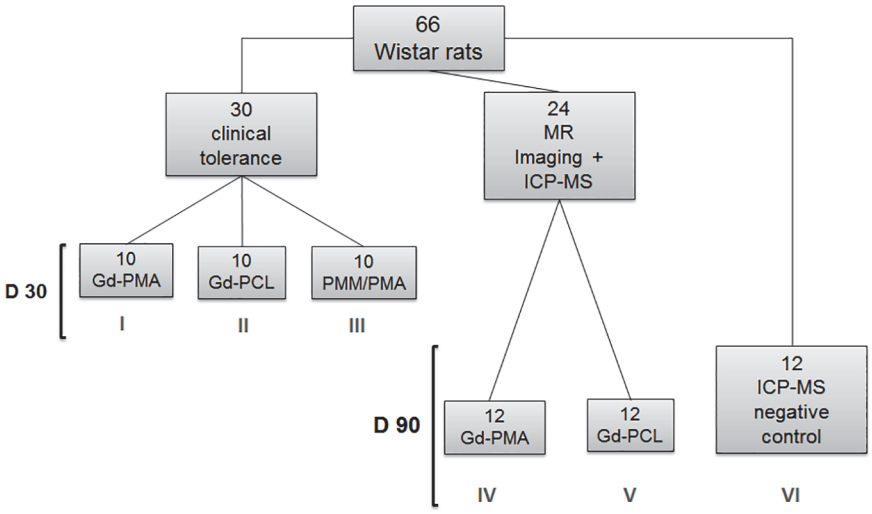

Fig 1. Flowchart showing experimental and control groups.

doi:10.1371/journal.pone.0120218.g001

anaesthetised with 2.5% halothane (0.5 L/min) and ketamine (50 mg/kg) and all efforts were made to minimise suffering.

A total of 66 Wistar rats (Charles River Laboratoires, L'Arbresle, France) were used during this study; all rats were randomised to one of the 6 groups of the study (see Fig. 1). For the tolerance experiments 30 rats were used: two test groups (Gd-PMA- experimental group I; and Gd-PCL experimental group II-modified meshes) and a control group (PMA/PMMA (poly (methyl methacrylate)) modified meshes—control group III) were analysed with ten rats allocated to each group; all meshes were implanted within the abdominal wall. The surgical procedure used is based on incisional abdominal hernia and has been previously described [21]. For MR imaging two test groups were analysed: Gd-PMA (experimental group IV) 12 rats and Gd-PCL (experimental group V) 12 rats. In each rat four meshes were implanted, two coated with Gd-complexes and two coated with PMA/PMMA. To this purpose subcutaneous dorsal implantations were performed: two 2-cm incisions were made on each side of the backbone, two pieces of Gd-complex mesh of 20 x 30 mm and 10 x 30 mm in size were implanted on the lumbar muscle on the left side and sutured. PMA/PMMA control meshes were similarly implanted but on the right side and sutured (Fig. 2). For both pairs, the meshes were placed at a millimetre distance. All animals that underwent surgery were assessed for signs of local (erosions) or systemic complications (infection) every day.

MRI analyses were performed at day 30 and day 90: before being placed in MRI devices, all animals were sedated. At day 90, after all imaging analyses were performed, animals were euthanised. The subcutaneous plane was initially exposed and the scar tissue over the mesh was examined. The inner surface of the mesh was then inspected via a U-shaped incision. None of the animals died during surgery. Lastly 12 rats, in which no mesh was implanted, were used as negative controls for gadolinium toxicity measures (experimental group VI). Rats were kept isolated for 3 days after operation then caged in pairs. Analgesic treatment was applied routinely once a day for 3 days after surgery by subcutaneous injection of Metacam 0.07 ml per 400 g bodyweight, as described before [12]. Death and presence of clinical signs of disease

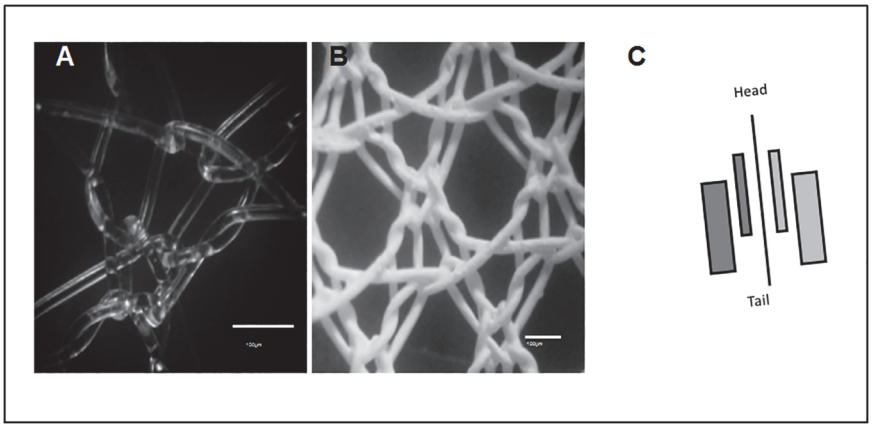

Fig 2. Microscopic view of the mesh. (A) Mesh before coating; (B) Gd-PMA Coated mesh as observed at an optical microscope (X100). (C) Schematic view of the implantation sites in rat: Gd-PMA coated mesh on the left (purple) and PMA/PMMA mesh (uncoated control) on the right side (blue).

doi:10.1371/journal.pone.0120218.g002

(weight, fur, presence if stools, signs of prostration and aggressiveness) were monitored daily by the animal housing operators and weekly by the veterinary surgeon.

Gd-PCL and Gd-PMA were coated onto PP mesh (manufacturer COVIDIEN, Trévoux, France) as described before [17].

Histology and immunohistochemistry

Thirty days after surgery (D = 30) prostheses were explanted and the entire anterior abdominal wall (from the skin until the peritoneum) was harvested. For each test group (Gd-PMA, Gd-PCL and control) three biopsies were collected. Each specimen was divided into two parts along the longitudinal axis (middle line Fig. 2C) in order to have specimens for histopathological and specimens for immunohistochemical analyses. For standard histological analysis, samples were fixed in formaldehyde (5%), dehydrated with double alcohol and toluene substitution, five tissue sections of 4 μm were collected for each sample (cut adjacently) and stained with Hematoxyline Eosine and Safran (HES) coloration. Immunohistochemistry for types I and III collagen was also performed: specimens were frozen in liquid nitrogen and then stored at −80°C, five slices of 10 μm (cut adjacently) were obtained at the cryomicrotome and then fixed in acetone. Analysis of extracellular matrix was carried out by labelling type I and III collagens with rabbit anti-rat collagen I (abcam #ab24133) at 1:250 dilutions and rabbit anti-rat collagen III (abcam #ab7778) at 1:200 dilutions. For the analysis of vascularisation smooth muscle α-actin was labelled with anti-rat antibody (abcam #ab5694) at 1:200 dilution. The secondary antibodies used were peroxidase-conjugated Affinipure Goat anti-rabbit (111–035–144); peroxidase-conjugated Affinipure Goat anti-mouse (115–035–146) (both purchased from Jackson Immuno Research).

All histology and immunohistochemistry analyses were performed with a Leica Optical Microscope at 40X magnification.

MR imaging

We sought to optimise the MRI sequences to visualise the polymer-coated mesh. The objective was to obtain a T1- weighted image. As first step, experimental (7T) MRI (Bruker Avance DRX system) was used to obtain high resolution 3D images of Gd-PCL and Gd-PMA coated meshes.

Images were acquired with standard T1-weighted fast spoiled gradient recalled echo (FSPGR) [17].

To define and optimise sequences for visualisation of meshes *in vivo*, coated implants were embedded in 1% w/w low gelling point agarose type VII (Sigma Aldrich, France) or inserted in muscle tissue within 20mL disposable scintillation glass vials (Dutcher, France) and then placed in 3T MRI (GE Healthcare) devices for analysis. Gradient echo sequence, routinely used in clinical practice for the exploration of the pelvis, was used. In order to assure reproducibility, the best sequences obtained for both 3T and 7T (3D T1-weighted spoiled gradient echo images were acquired with TR/TE = 100/3ms, alpha = 75°, a field-of-view of 30x30x10 mm3 and a matrix of 64x64x32 matrix. Two averages were performed leading to an imaging time of 11 min) were used to acquire all images. To verify the stability of the coated meshes, samples were stored up to one year at 37°C and tested for imaging at 4 months and one year, the size of the mesh was measured at every imaging assay. The reconstruction of images obtained was performed using the 3D reconstruction software OsiriX.

Toxicity measures

The validation of the stability of the Gd-polymers was confirmed by assaying the diffusion of gadolinium by inductively coupled plasma mass spectrometry (ICP-MS) [22,23]. The ICP-MS allows us to measure the amount of gadolinium in organs after mesh implantation. Peripheral and systemic distribution of gadolinium toxicity was assessed in implanted rats and compared to control group (at D90). To detect gadolinium accumulation in organs: liver and kidney tissues were harvested and processed. A few milligrams of the samples were weighed and dissolved with concentrated nitric acid in suprapure quality (Merck, Darmstadt, Germany) in a glass tube at 80°C. For calibration, a gadolinium standard solution was diluted with deionized water to obtain calibration solutions. ICP-MS operating conditions were optimized to obtain the highest signal-to-background ratio for gadolinium, the isotope that was applied for the analytical determination.

Statistical Analyses

The number of animals was based on published studies [24,25]. All statistical analyses were performed with SAS (version 8) statistical software. Data are expressed as mean ± standard deviations (SD). Statistical significance of differences among groups (implanted vs control groups) was evaluated with a t-test with level of significance set at $P<0.05$.

Results

Clinical Tolerance of Gd-Polymers coated mesh

The evaluation of the clinical tolerance on an animal model and the non-systemic diffusion of Gadolinium are essential features to meet the pre-clinical characteristics of the implant.

At three months after implantation, the healing process was completely achieved for the animals implanted with Gd-PMA and PMA/PMMA meshes while rats implanted with Gd-PCL meshes displayed a noticeable erosion rate (100% (n = 10/10) Gd-PCL vs 0% (n = 0/10) Gd-PMA) as shown in Fig. 3. Mean apparition of the erosion on PCL meshes was at 21±3 days.

Microscopic analysis of histology sections showed mild inflammation for the non-coated mesh and Gd-PMA coated mesh groups. For both these groups the tissue surrounding the implants was characterised by the presence of non-inflammatory collagen and important blood supply. For the Gd-PMA group in particular, substantial neoangiogenesis with capillaries and venules could be observed. For the non-coated mesh group, the tissue was also characterised by

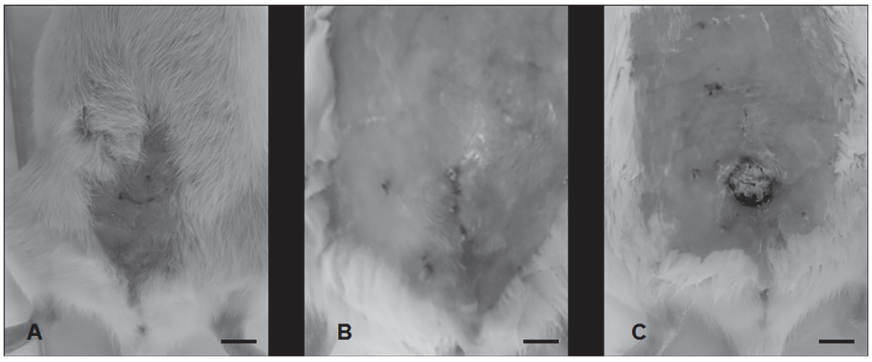

Fig 3. Postoperative inspection of the rats. Clinical observation at day 30. Representative images of (A) Non-coated PP mesh control group (III); (B) Gd-PMA coated mesh experimental group (I) and (C) Gd-PCL coated mesh experimental group (II). Erosion was visible only on Gd-PCL implanted group. Scale bars: (A) 1cm, (B) 2mm an (C) 0,8cm.

doi:10.1371/journal.pone.0120218.g003

the presence of myofibroblasts with good mesenchymal organisation. On the other hand tissues surrounding Gd-PCL coated mesh were characterised by the presence of disordered collagen, persistent cellular inflammation and giant cell granulomas. Also, low levels of neo angiogenesis were visible (Fig. 4).

Immunohistochemistry showed similar patterns of smooth muscle α-actin, types I and III collagen between non-coated and Gd-PMA coated mesh groups. In particular, for the non-coated mesh group we could observe well organised blood vessels, which were no longer capillaries but mainly venules and arterioles. For the Gd-PMA group blood vessels were organised in an intermediary structure (few capillaries and mostly venules and arterioles). Tissues from Gd-PCL implanted rats show a high level of inflammation with few blood vessels mainly capillaries. Types I and III staining showed a good extracellular matrix organisation for the uncoated and Gd-PMA coated implants with a higher amount of collagen I compared to collagen III. For the Gd-PCL on the contrary, very low levels of collagen I were visible (Fig. 4).

In vivo imaging

For imaging of the coated meshes both experimental 7T and clinical 3T were used. Due to the very poor tolerance of Gd-PCL meshes, animals implanted with these implants were excluded from imaging assays.

With both techniques we obtained a clear visualisation of a Gd-PMA mesh coated at a dose of 3.8 μg / cm^2. Coated meshes were visible with both 3T and 7T MRI techniques. All meshes were entirely a homogenously visible; indeed, the size of the mesh (image) corresponded to the size of the mesh *in vivo*.

3D reconstruction program allowed the optimisation of MR imaging by highlighting the contrast of the mesh and therefore allowing us to distinguish the implant within the different muscular layers (Figs. 5 and 6).

In vivo toxicity evaluation

The ICP-MS evaluation after degradation of explanted meshes allowed to measure residual doses of gadolinium in surrounding tissues and in the organs metabolising Gd. The concentrations were measured in liver, kidney, tibia bone and skin of the animals implanted with coated meshes. No significant differences in mean levels of gadolinium were found in implanted group as compared to control group (Table 1).

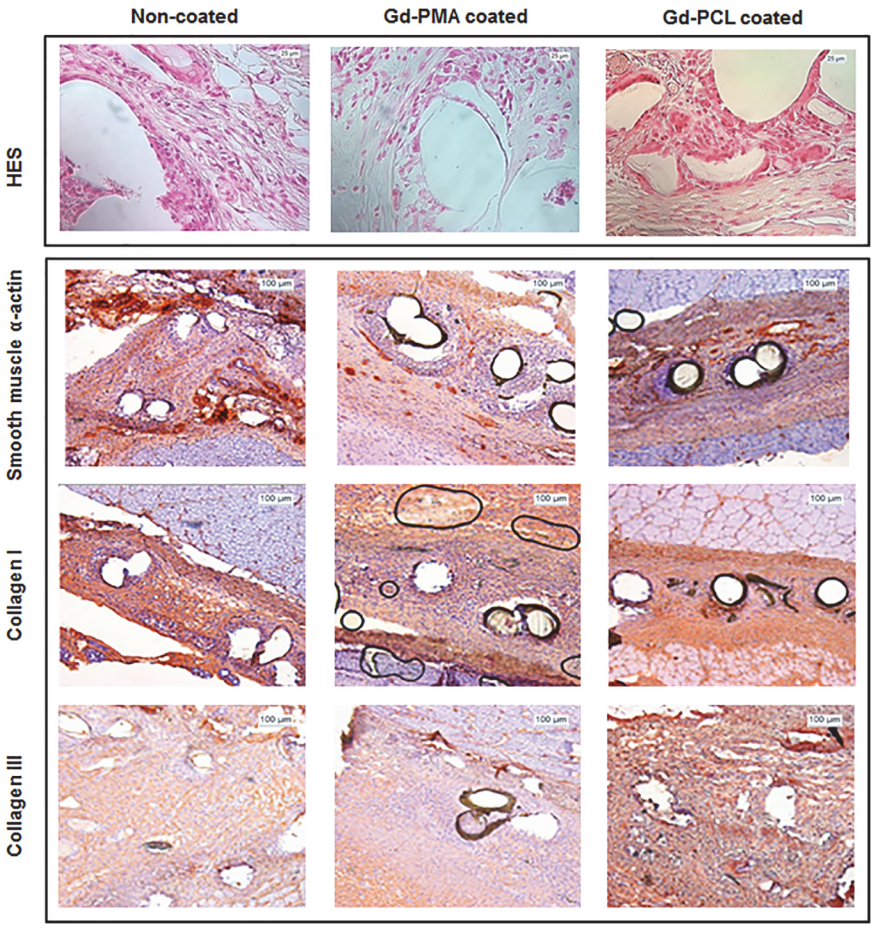

Fig 4. Histological images of the explanted meshes. Upper panel: Standard histological results at day 30 of Hematoxyline Eosine and Safran (HES) stained sections of non-coated mesh (control group I), Gd-PMA coated mesh (experimental group II) and Gd-PCL coated mesh (experimental group III). Lower panel: Immuno-histochemistry sections of non-coated mesh (control group I), Gd-PMA coated mesh (experimental group II) and Gd-PCL coated mesh (experimental group III) labelled for smooth muscle α-actin, collagen I and collagen type III (Optical microscope X40 magnification).

doi:10.1371/journal.pone.0120218.g004

Discussion

With this study we sought to evaluate the tolerance and long-term MRI visibility of Gadolinium-modified polypropylene meshes for their use in soft tissue repair.

Appropriate modification of the meshes used for reinforcing the tissues in pelvic organ disorders enables their visualisation on magnetic resonance imaging [17]. This technology may represent an essential feature to optimise the management of complications and the recurrence of soft tissue and therefore its surgical management. The follow-up by ultrasound techniques has been previously investigated but their use has been restricted to the visualisation of meshes only in the vaginal segment. At the same time MRI has emerged as the tool of choice for monitoring implantation of meshes in the tissues [26–28]. Hansen and colleagues showed that iron particles incorporated into polymer-based implants allow MRI visualisation and offer a non-invasive alternative to surgical exploration in case of suspected mesh-related complications [27]. The exploration of the pelvis by MRI provides a lot of useful information for the pre and postoperative monitoring of all gynaecological pathologies requiring surgical management. Initially used for neuroradiology applications, 3T high-field MRI was quickly adopted in many

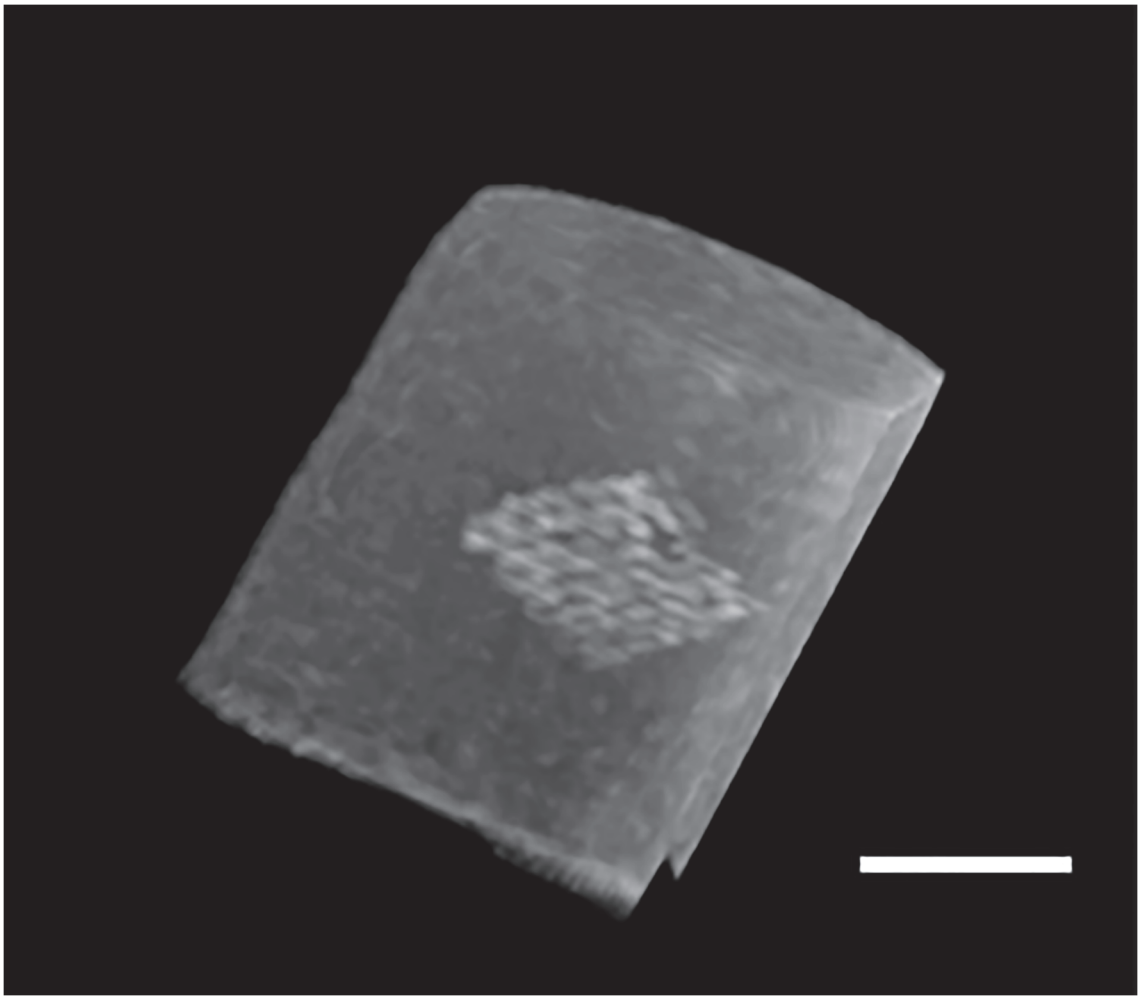

Fig 5. MRI images of the mesh in vitro. Gd-PMA coated mesh with a 3T MRI device, reconstruction was obtained with osiriX software. Scale bar 1 cm.

doi:10.1371/journal.pone.0120218.g005

scientific and clinical domains such as uro-gynaecology [29]. Previous studies showed that MRI-visible polymer (DTPA-Gd-PCL) coated onto PP meshes enables *in vitro* visualisation of the mesh for at least one year [30]. Also, Gd-PMA coated meshes revealed good level of

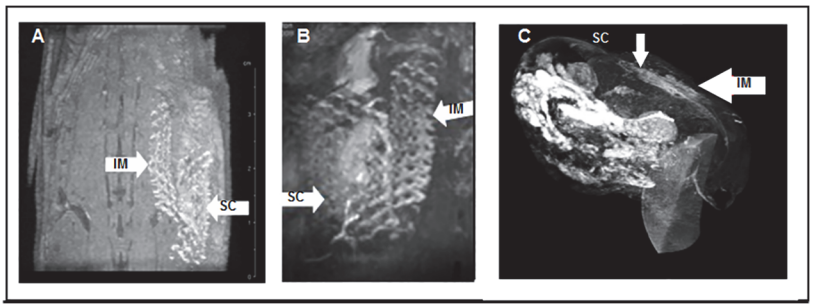

Fig 6. In vivo visualisation of the mesh. (A) Frontal and **(B)** lateral view of Gd-PMA coated meshes as seen with a 7T MRI device, 3D reconstruction was obtained with OsiriX software. **(C)** 3D reconstruction of a Gd-PMA coated mesh (dorsal implantation) (3T MRI). Note MRI imaging and 3D reconstruction allow us to distinguish between two meshes (arrows) implanted subcutaneously (SC) and intramuscularly (IM) within few millimetres distance. Scale bars in A and C 1cm, B 5mm.

doi:10.1371/journal.pone.0120218.g006

Table 1. Gadolinium concentrations (ppm) measured in rats implanted with coated meshes (implanted group) and not-implanted (control group).

Organs	Implanted group (n = 12)	Control group (n = 12)
Liver	0.17±0.08	0.17±0.02
Kidney	0.09±0.02	0.07±0.02
Tibia bone	0.05±0.02	0.12±0.03
Skin	0.09±0.02	0.09±0.01

doi:10.1371/journal.pone.0120218.t001

cytocompatibility [14]. With this study we aimed to compare both polymer (PMA and PCL) not only in terms of in vivo long-term MRI-visibility but also in terms of biocompatibility and in vivo tolerance. Interestingly, in vitro results, which suggested PCL as equally good polymer for gadolinium linking to a PP mesh, were not supported by in vivo experiments and clinical observations. A possible explanation of high level of erosion observed in Gd-PCL implanted rats may be that these polymers release acid products upon biodegradation that may lead to inflammatory reactions and eventually tissue necrosis [31]. In this study we showed that Gd-PMA does not provoke any erosion, allows a good integration of the implant with low levels of inflammation, a suitable extracellular matrix organisation and vascularisation of the integration tissues. A limitation of this study is that only visual inspection was performed on the HES and IHC sections without a precise scoring. However, as the erosion provoked by of the Gd-PCL implants was observed before the histological analyses could be performed; the scoring was not considered to add valuable information. All together these observations suggest that PMA is a linking polymer suitable for implantable devices modification. PP was chosen as standard support material, but Gd-PMA linking technique may as well be extended to other biomaterials used to synthesise meshes.

Gadolinium was not the only MRI contrast agent that may have been selected for this purpose. Fluorinated derivatives have been exploited before [32], but resulting images consisted only in a hyposignal therefore reducing the interest in pelvis MR imaging.

The MRI visualisation was obtained in vitro for both types of polymers (Gd-PCL and Gd-PMA), but the intensity of the signal observed was stronger with PMA than with PCL, probably because of its hydrophilic nature. As discussed above, the cutaneous and tissular integration was not clinically satisfactory in the case of the Gd-PCL implants confirming that Gd-PMA were more suitable for further investigation.

The amount of gadolinium necessary for mesh imaging is correlated to the type of MRI, the tissues surrounding the area of the implants and their intrinsic contrasts. Results from previous studies helped to reinforce the idea that low doses of gadolinium are necessary (ranging from 1 to 20μg / cm2 according to the type of MRI used) [29].

In vivo MR imaging raises the issue of the implant precise location and the risk of confusion with many artefacts due to the production of millimetre slices. The imaging artefacts, such as respiratory movements of animals, may hamper the image optimisation in abdominal position. On the contrary, the dorsal implantation of the mesh allowed us to precisely locate two very close (mm distance) implants. Nevertheless, these distances may entail more artefacts; discrimination of such artefact was however confirmed by accurate 3D images reconstruction (Fig. 6).

Experimental studies on the rat model requires many volume settings directly related to the size of the animal and therefore to the sample. For instance, standard settings in clinical MRI allow us to obtain cuts of 5mm. Because of the millimetre range of meshes it was necessary to reduce the thickness to 3 mm as well as to adapt the sequences. Pre-sets and standardised parameters in 3T MRI adapted to clinical situations do not exist on 7T MRI where each parameter is defined independently. It is therefore difficult to establish correspondences between

clinical and experimental MRI. Another limitation of this study is represented by the animal model itself: the time period during which rats may be followed is limited to three months, which does not allow extrapolation to humans and conclusion about the long-term (years) effects of the implants. This problem may be only partially overcome by testing the Gd-modified meshes on a bigger (ovine) model which allow a longer follow-up period.

Nephrogenic systemic fibrosis (NSF) induced by Gadolinium-based contrast agent, has been described in rats, mainly in the dermic tissue [22]. Hence, it is important to be able to determine the presence of free Gadolinium in tissues immediately adjacent to the implanted mesh, in skin and various organs (liver and kidney) [22]. ICP-MS is a type of mass spectrometry capable of detecting very low concentrations of metal with greater precision and sensitivity as compared to spectroscopic techniques [23]. ICP-MS assays performed on tissues harvested from implanted animals, have highlighted the absence of diffusion of Gadolinium and therefore minimal risk of nephrogenic systemic fibrosis.

The last decades have seen a remarkable growth in the applications of MR imaging. The need for the visualisation of meshes used in pelvic floor surgery derives directly from the necessity to optimise the monitoring and care of patients. The stability of the Gd-complex coated meshes allows the visualisation over time of the implants. By linking the clinical symptoms to the observation of an anatomical region will result in the improved management of complications. Monitoring of the mesh would allow clinicians to assign responsibility for a post-operative symptom. In conclusion, the technique described above allows a non-invasive and long-term imaging of implants.

Acknowledgments

The authors would like to thank Dr Mariella Lomma, Dr Daniela Ulrich and Dr Pierre Rataboul (Dept of Epidemiology and Biostatistics, Nimes University Hospital) for their medical editorial assistance and Dr. Florence Franconi for her MRI technical support.

Author Contributions

Conceived and designed the experiments: XG VL. Performed the experiments: SH SB OG AC LL. Analyzed the data: VL XG RdT. Contributed reagents/materials/analysis tools: VL SH SB AC LL. Wrote the paper: VL SH XG RdT.

References

1. Wolstenholme JT. Use of commercial dacron fabric in the repair of inguinal hernias and abdominal wall defects. AMA Arch Surg. 1956; 73: 1004–1008. PMID: 13372032
2. Maher C, Baessler K, Glazener CMA, Adams EJ, Hagen S. Surgical management of pelvic organ prolapse in women. Cochrane Database Syst Rev. 2007; CD004014. doi: 10.1002/14651858.CD004014.pub3
3. Letouzey V, Deffieux X, Gervaise A, Mercier G, Fernandez H, de Tayrac R. Trans-vaginal cystocele repair using a tension-free polypropylene mesh: more than 5 years of follow-up. Eur J Obstet Gynecol Reprod Biol. 2010; 151: 101–105. doi: 10.1016/j.ejogrb.2010.03.013 PMID: 20417020
4. Amid PK, Shulman AG, Lichtenstein IL, Hakakha M. Biomaterials for abdominal wall hernia surgery and principles of their applications. Langenbecks Arch Für Chir. 1994; 379: 168–171.
5. Coda A, Lamberti R, Martorana S. Classification of prosthetics used in hernia repair based on weight and biomaterial. Hernia J Hernias Abdom Wall Surg. 2012; 16: 9–20. doi: 10.1007/s10029-011-0868-z
6. Birch C, Fynes MM. The role of synthetic and biological prostheses in reconstructive pelvic floor surgery. Curr Opin Obstet Gynecol. 2002; 14: 527–535. PMID: 12401983
7. Bellón JM, García-Carranza A, García-Honduvilla N, Carrera-San Martín A, Buján J. Tissue integration and biomechanical behaviour of contaminated experimental polypropylene and expanded polytetrafluoroethylene implants. Br J Surg. 2004; 91: 489–494. doi: 10.1002/bjs.4451 PMID: 15048754

8. Sivaslioglu AA, Unlubilgin E, Dolen I. A randomized comparison of polypropylene mesh surgery with site-specific surgery in the treatment of cystocoele. Int Urogynecol J Pelvic Floor Dysfunct. 2008; 19: 467–471. doi: 10.1007/s00192-007-0465-y PMID: 17901910
9. De Tayrac R, Letouzey V. Basic science and clinical aspects of mesh infection in pelvic floor reconstructive surgery. Int Urogynecology J. 2011; 22: 775–780. doi: 10.1007/s00192-011-1405-4 PMID: 21512828
10. Jia X, Glazener C, Mowatt G, MacLennan G, Bain C, Fraser C, et al. Efficacy and safety of using mesh or grafts in surgery for anterior and/or posterior vaginal wall prolapse: systematic review and meta-analysis. BJOG Int J Obstet Gynaecol. 2008; 115: 1350–1361. doi: 10.1111/j.1471-0528.2008.01845.x
11. Altman D, Väyrynen T, Engh ME, Axelsen S, Falconer C, Nordic Transvaginal Mesh Group. Anterior colporrhaphy versus transvaginal mesh for pelvic-organ prolapse. N Engl J Med. 2011; 364: 1826–1836. doi: 10.1056/NEJMoa1009521 PMID: 21561348
12. Gruber-Blum S, Petter-Puchner AH, Brand J, Fortelny RH, Walder N, Oehlinger W, et al. Comparison of three separate antiadhesive barriers for intraperitoneal onlay mesh hernia repair in an experimental model. Br J Surg. 2011; 98: 442–449. doi: 10.1002/bjs.7334 PMID: 21254024
13. García-Moreno F, Sotomayor S, Pérez-López P, Pérez-Köhler B, Bayon Y, Pascual G, et al. Intraperitoneal behaviour of a new composite mesh (Parietex™ Composite Ventral Patch) designed for umbilical or epigastric hernia repair. Surg Endosc. 2014; doi: 10.1007/s00464-014-3633-4
14. Onal S, Lai-Yuen S, Bao P, Weitzenfeld A, Greene K, Kedar R, et al. Assessment of a semiautomated pelvic floor measurement model for evaluating pelvic organ prolapse on MRI. Int Urogynecology J. 2014; 25: 767–773. doi: 10.1007/s00192-013-2287-4 PMID: 24429795
15. Alt CD, Brocker KA, Lenz F, Sohn C, Kauczor H-U, Hallscheidt P. MRI findings before and after prolapse surgery. Acta Radiol Stockh Swed 1987. 2014; 55: 495–504. doi: 10.1177/0284185113497201
16. Paine M, Harnsberger JR, Whiteside JL. Transrectal mesh erosion remote from sacrocolpopexy: management and comment. Am J Obstet Gynecol. 2010; 203: e11–13. doi: 10.1016/j.ajog.2010.04.028 PMID: 20579965
17. Guillaume O, Blanquer S, Letouzey V, Cornille A, Huberlant S, Lemaire L, et al. Permanent polymer coating for in vivo MRI visualization of tissue reinforcement prostheses. Macromol Biosci. 2012; 12: 1364–1374. doi: 10.1002/mabi.201200208 PMID: 22887855
18. Reijnen MJ, Meis JM, Postma VA, van Goor H. PRevention of intra-abdominal abscesses and adhesions using a hyaluronic acid solution in a rat peritonitis model. Arch Surg. 1999; 134: 997–1001. doi: 10.1001/archsurg.134.9.997 PMID: 10487596
19. Harth KC, Blatnik JA, Anderson JM, Jacobs MR, Zeinali F, Rosen MJ. Effect of surgical wound classification on biologic graft performance in complex hernia repair: an experimental study. Surgery. 2013; 153: 481–492. doi: 10.1016/j.surg.2012.08.064 PMID: 23218885
20. Pascual G, Hernández-Gascón B, Rodríguez M, Sotomayor S, Peña E, Calvo B, et al. The long-term behavior of lightweight and heavyweight meshes used to repair abdominal wall defects is determined by the host tissue repair process provoked by the mesh. Surgery. 2012; 152: 886–895. doi: 10.1016/j.surg.2012.03.009 PMID: 22575883
21. Mamy L, Letouzey V, Lavigne J-P, Garric X, Gondry J, Mares P, et al. Correlation between shrinkage and infection of implanted synthetic meshes using an animal model of mesh infection. Int Urogynecology J. 2011; 22: 47–52. doi: 10.1007/s00192-010-1245-7 PMID: 20821311
22. Boyd AS, Sanyal S, Abraham JL. Tissue gadolinium deposition and fibrosis mimicking nephrogenic systemic fibrosis (NSF)-subclinical nephrogenic systemic fibrosis? J Am Acad Dermatol. 2010; 62: 337–342. doi: 10.1016/j.jaad.2009.04.010 PMID: 19939504
23. White GW, Gibby WA, Tweedle MF. Comparison of Gd(DTPA-BMA) (Omniscan) versus Gd(HP-DO3A) (ProHance) relative to gadolinium retention in human bone tissue by inductively coupled plasma mass spectroscopy. Invest Radiol. 2006; 41: 272–278. doi: 10.1097/01.rli.0000186569.32408.95 PMID: 16481910
24. Szabo A, Haj M, Waxsman I, Eitan A. Evaluation of Seprafilm and Amniotic Membrane as Adhesion Prophylaxis in Mesh Repair of Abdominal Wall Hernia in Rats. Eur Surg Res. 2000; 32: 125–128. doi: 10.1159/000008751 PMID: 10810219
25. Hellebrekers BWJ, Trimbos-Kemper GCM, van Blitterswijk CA, Bakkum EA, Trimbos JBMZ. Effects of five different barrier materials on postsurgical adhesion formation in the rat. Hum Reprod. 2000; 15: 1358–1363. doi: 10.1093/humrep/15.6.1358 PMID: 10831569
26. Fischer T, Ladurner R, Gangkofer A, Mussack T, Reiser M, Lienemann A. Functional cine MRI of the abdomen for the assessment of implanted synthetic mesh in patients after incisional hernia repair: initial results. Eur Radiol. 2007; 17: 3123–3129. doi: 10.1007/s00330-007-0678-y PMID: 17549486

27. Hansen NL, Barabasch A, Distelmaier M, Ciritsis A, Kuehnert N, Otto J, et al. First in-human magnetic resonance visualization of surgical mesh implants for inguinal hernia treatment. Invest Radiol. 2013; 48: 770–778. doi: 10.1097/RLI.0b013e31829806ce PMID: 23732864

28. Franconi F, Roux J, Garric X, Lemaire L. Early postsurgical visualization of composite mesh used in ventral hernia repair by amide proton transfer MRI. Magn Reson Med Off J Soc Magn Reson Med Soc Magn Reson Med. 2014; 71: 313–317. doi: 10.1002/mrm.24666

29. Willinek WA, Schild HH. Clinical advantages of 3.0 T MRI over 1.5 T. Eur J Radiol. 2008; 65: 2–14. doi: 10.1016/j.ejrad.2007.11.006 PMID: 18162354

30. Blanquer S, Guillaume O, Letouzey V, Lemaire L, Franconi F, Paniagua C, et al. New magnetic-resonance-imaging-visible poly(ε-caprolactone)-based polyester for biomedical applications. Acta Biomater. 2012; 8: 1339–1347. doi: 10.1016/j.actbio.2011.11.009 PMID: 22115697

31. Ali SA, Zhong SP, Doherty PJ, Williams DF. Mechanisms of polymer degradation in implantable devices. I. Poly(caprolactone). Biomaterials. 1993; 14: 648–656. PMID: 8399961

32. Romero-Aburto R, Narayanan TN, Nagaoka Y, Hasumura T, Mitcham TM, Fukuda T, et al. Fluorinated graphene oxide; a new multimodal material for biological applications. Adv Mater Deerfield Beach Fla. 2013; 25: 5632–5637. doi: 10.1002/adma201301804 PMID: 24038195